2022 International Symposium on Nonlinear Theory and Its Applications,
NOLTA2022, Virtual, December 12-15, 2022

Modeling of dynamics of nonlinear wave propagation in phononic crystals

Jun Takayanagi†, Yusuke Doi†, and Akihiro Nakatani†

†Division of Mechanical Engineering, Graduate School of Engineering, Osaka University
2-1 Yamadaoka, Suita, Osaka 565-0871, Japan
Email: takayanagi@md.mech.eng.osaka-u.ac.jp, doi@mech.eng.osaka-u.ac.jp, nakatani@mech.eng.osaka-u.ac.jp

Abstract—We construct a nonlinear lattice model to investigate the dynamics of nonlinear behavior in phononic crystals (PnCs). Two types of mass points and springs are introduced in the model to reproduce the difference in material properties between the scatterers and background in PnCs. The nonlinearity is introduced to the model by changing the mass of each mass point depending on the displacement gradient at the mass point. We confirm that both the 1D and 2D models have the bandgap in the linear dispersion relation. Moreover, in the 1D nonlinear model, switching behavior of wave propagation is found.

1. Introduction

Metamaterials are artificial materials, which are getting more attention for their interesting properties. A lot of metamaterials have complicated internal structure, which leads to properties which natural materials never have. These properties are expected to be widely used for human technology, such as, noise controlling, heat transfer controlling. Nonlinearity in metamaterials has been attracting attention in recent years due to its potential to add new properties and functions to metamaterials.

Phononic crystal (PnC) is a type of metamaterials consisting of background and scatterers embedded in the background. The PnCs have phononic band gap (PnBG) in which wave cannot propagate. Due to the PnBG, the PnCs are expected to be used for wide applications, such as, energy transduction, and thermal transportation[1][2].

Moreover, new properties have been realized by applying the nonlinear dynamics in the PnC. For example, it has been reported that the PnC can realize switching behavior by combining the PnBG and nonlinear wave propagation[3][4][5]. The switching structure (SS), which has a structure in which the PnC scatterers are partially replaced with scatterers with different property can realize switching only at certain frequency called switching frequency. In the SS, wave does not propagate when the amplitude of the wave is increased at switching frequency. The SS is expected to be applied to logic gates. However, the mechanism of this nonlinear behavior has not been clarified. To put SS to practical use, it is necessary to understand the mechanism of nonlinear behavior.

ORCID iDs Jun Takayanagi: 0000-0002-8926-3514, Yusuke Doi: 0000-0003-3749-5353, Akihiro Nakatani: 0000-0001-7212-9303

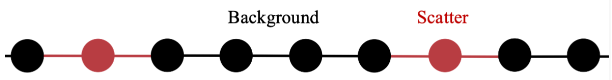

Figure 1: 1D model

In this study, we construct a nonlinear dynamics model of PnCs and the SS and we perform numerical simulations on these models to understand this nonlinear behavior. The left of the paper is organized as follows. In the section 2, we construct the model to reproduce the nonlinear behavior of the PnC and the SS. In the section 3, we perform numerical simulation in linear regime, and confirm the existence of band gap in the model. In section 4, we perform nonlinear dynamics simulation in the model to see whether switching behavior can be reproduced. Finally, a brief conclusion is given in section 5.

2. Constructing the dynamics model

In this section, we construct the model to reprodece the behavior of PnC and SS.

2.1. 1D model

We construct a nonlinear lattice model which reproduce the dynamics of the nonlinear PnC. Fig. 1 shows the 1D lattice model. The scatterers and the background materials of PnC have different material properties. This difference is models by introducing two types of mass point as well as two types of springs. The red mass points and springs in Fig. 1 indicate the part of scatterers. On the other hand, the black mass points and springs indicate the part of background materials. In this study, the mass points of the scatterer are 10 times larger than those of the background material, and the spring constant of the scatterer is 10^3 times larger than that of the background material. The nonlinearity of materials is modeled by introducing the nonlinear mass density which is a function of the displacement as

$$m_i(t) = M_i \frac{1}{1 + \nabla \cdot u_i(t)}, \tag{1}$$

where $u_i(t)$ is the displacement of i-th particle at time t, M_i is a reference mass of the i-th mass point at the equilibrium state. The divergence $\nabla \cdot u_i$ which represents the volumetric

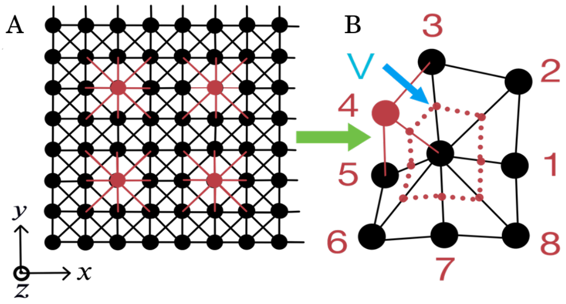

Figure 2: 2D model

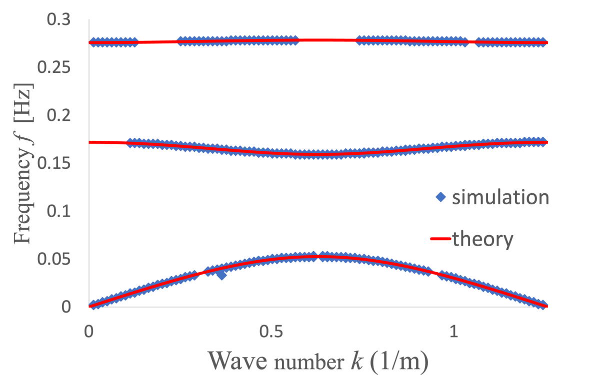

Figure 3: Dispersion relation of the 1D model: the red lines indicate theorical one, the blue squares indicates the numerical one from temporal evolution.

strain can be approximated as increment ϵ_i in 1D discrete model. ϵ_i is calculated as

$$\epsilon_i = \frac{u_{i+1} - u_{i-1}}{2l_0}, \tag{2}$$

where l_0 is the lattice constant.

The equations of motion of the i-th mass point is

$$M_i \frac{1}{1+\epsilon_i} \ddot{u}_i = -k_{i-1}(u_i - u_{i-1}) - k_i(u_i - u_{i+1}). \tag{3}$$

2.2. 2D model

We also construct the 2D lattice model as shown in Fig. 2. We consider a square lattice model. Each particle is connected to the eight adjacent particles. The scatterer pass points are embedded periodically in both x- and y- directions. In the 2D lattice model, the nonlinear mass is models as

$$m_{i,j} = M_{i,j}\frac{V_0}{V}, \tag{4}$$

where i, j are the indices in the x, y directions respectively, $M_{i,j}$ is a reference mass of the (i, j)-th mass point at the equilibrium state, volume $V_{i,j}$ of the (i, j)-th lattice is the area of octagon made of the eight surrounding mass points, $V_0 = l_0^2$ is a area of the square at the equilibrium state.

The equations of motion of the (i, j)-th mass point in x direction is

$$M_{i,j}\frac{V_0}{V}\ddot{u}_{i,j} = \sum_{s=1}^{8} F_s \cos\theta_s, \tag{5}$$

$$F_s = k_s(l_s - l_{s,0}). \tag{6}$$

In Eq. (5), F_s represents the force applied from the spring s in the Fig. 2B, θ_s the angle between x direction and spring s. In Eq. (6), k_s represents the spring constant of spring s, l_s length of spring s, $l_{s,0}$ the reference length of the spring s at the equilibrium state

3. Linear analysis

In this section, we analysis the behavior of the model in linear regime, which means mass of each mass points in the model remain the initial value. We confirm the existence of band gap in the model.

3.1. 1D model

In the 1D model, we confirm the existence of band gap by analyzing the dispersion relation between the wave number k and the frequency f. In the numerical simulation, scatterer mass points are placed every five index i, lattice constant $l_0 = 1.0$, and number of mass points N in the model is 500, and periodic boundary conditions apply.

3.1.1. Theory

The equation of motion (3) can be linearized by

$$M_i\ddot{u}_i = -k_{i-1}(u_i - u_{i-1}) - k_i(u_i - u_{i+1}). \tag{7}$$

Given the condition of the model, we can calculate the theorical disperison curves in the model based on the assumption that

$$u_{5n+s} = \alpha_s \exp\{i(\omega t - k[5n+s])\}, \tag{8}$$

where $n = 0, 1, 2 \ldots, s = 1 - 5$, ω is angular frequency. The dispersion curves are shown as solid lines in Fig. 3.

3.1.2. Numerical simulation

Numerical integration of Eq. (7) is performed in order to confirm the linear dispersion relation written in sec.3.1.1. The initial condition is given by

$$u_i(0) = a_0 \sin\left(j\frac{2\pi}{N}i\right), \tag{9}$$

where $a_0 = 0.001l_0$ is amplitude of initial displacement, $j = kN/2\pi$ varies from 1 to 100. The blue points in Fig. 3 indicates the angular frequency $\omega(k)$ estimated from the temporal evolution of vibrations of particle with initial conditions of wavenumber k. It is found that the theoretical and numerical results are almost identical. Thus, we have confirmed the existence of band gap at 0.053 - 0.159 [Hz] and 0.172 - 0.276 [Hz].

3.2. 2D model

The dispersion relation wavenumber (k_x, k_y) - angular frequency ω of the 2D model is confirmed by comparing the results of linear theory and linear simulation at small displacements for the two-dimensional model as well. In the following linear theory and simulation, the scatterer mass points are placed every 5 in the x and y directions, the lattice constant in each direction $l_0 = 10^{-1}$, the number of mass points in each direction is $n_x = n_y = 500$, and the periodic boundary condition is applied in each direction.

3.2.1. Theory

In case that the displacement of each mass point is small compared with the lattice constant l_0, θ_s is assumed constant, $\theta_s \sim \pi s/4$ $(s = 1-8)$. From above assumption, F_s in Eq. (6) can be approximated as

$$F_s \approx k_s \frac{\vec{l}_{s,0} \cdot \vec{u}_s}{l_{s,0}}, \tag{10}$$

where $\vec{u}_s$ is the displacement vector of adjacent mass point s from its equilibrium position and $\vec{l}_{s,0}$ is the position vector of mass point s from the equilibrium position of mass point (i, j). Suppose that the displacement of each mass point in the 2D model is represented by

$$\vec{u}_{i,j} = \begin{pmatrix} a_{i,j} \\ b_{i,j} \end{pmatrix} \exp\left\{ \boldsymbol{k} \cdot \begin{pmatrix} i \\ j \end{pmatrix} + \omega t \right\}, \tag{11}$$

where $\boldsymbol{k} = (k_x, k_y)$ is wavenumber vector. The amplitudes of the displacements of each mass point in the $x-$ and $y-$ directions are given by $a_{i,j}$,$b_{i,j}$, which are 5 periodic in each direction from the periodicity of the model, that is, $(a_{5\alpha+\gamma,5\beta+\delta}, b_{5\alpha+\gamma,5\beta+\delta}) = (a_{\gamma,\delta}, b_{\gamma,\delta})$. Based on the above conditions for amplitude, we derive a theoretical dispersion relation k - frequency $f(= \omega/2\pi)$ that simultaneously satisfies (model periodicity in $x-$ direction) 5 $\times$ (model periodicity in $x-$ direction)5 $\times$ (number of dimension) 2 equations of motion. The results are shown as solid gray lines in Fig. 4.

3.2.2. Numerical simulation

Next, a linear simulation is performed to derive the dispersion relation in the 2D model and compare it with the theoretical dispersion relation derived from the linear theory. In the linear simulation, initial displacements

$$\vec{u}_{i,j} = \begin{pmatrix} a_0 \\ a_0 \end{pmatrix} \sin\left\{ \frac{2\pi w}{n_x} i + \frac{2\pi \cdot 0}{n_y} j \right\} \tag{12}$$

is given, where $a_0 = 0.01 l_0$ is the amplitude of initial displacement in $x-$ and $y-$ directions, w is varied from 1 - 50. wavenumber in the $x-$ direction k_x, caluculated by $2\pi w/n_x$ is varied from $0 - 0.628$.

The results of the simulation are shown in Fig. 4 with blue dots. The linear theory and simulation results do not match for results around $f = 4.6$[Hz] and for $f > 5.5$[Hz]. This may be caused by accuracy of the linear theory. However, the results agree with the linear theory in that the band gap is around $0.4 - 4.2$[Hz] and that there is a dispersion relation at $f = 4.2$ and 5.0[Hz].

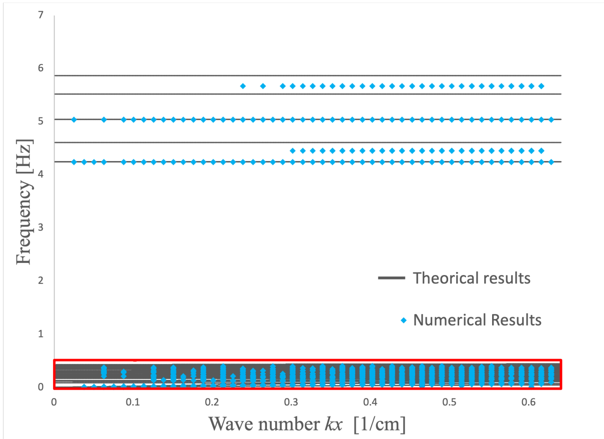

Figure 4: Dispersion relation of the 2D model: the grayed lines indicate theorical one, the blue dots indicates the numerical one from temporal evolution. Results of the part surrounded by the red frame is shown in Fig. 5.

Fig.5 shows the results under 0.5 [Hz], the red frame shown in Fig. 4. The correspondence with the linear theory could not be confirmed for this frequency range due to the low resolution of the Fourier transform of the linear simulation.

4. Nonlinear dynamics modeling

We introduce the nonlinearity in the 1D model, and see how the nonlinearity affect to dispersion relation, and whether switching behavior can be realized in the model. In numerical simulation, sinusoidal initial displacement is

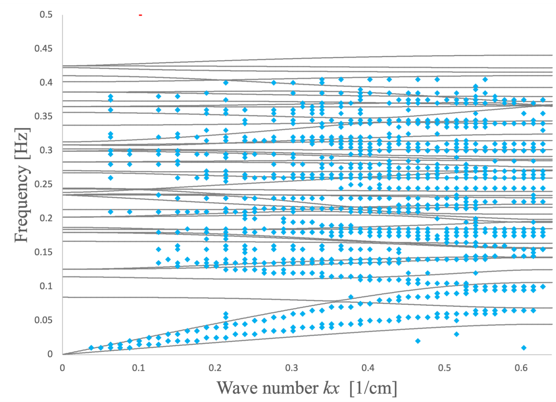

Figure 5: Dispersion relation of 2D model in the frequency range $f < 0.5$ [Hz]

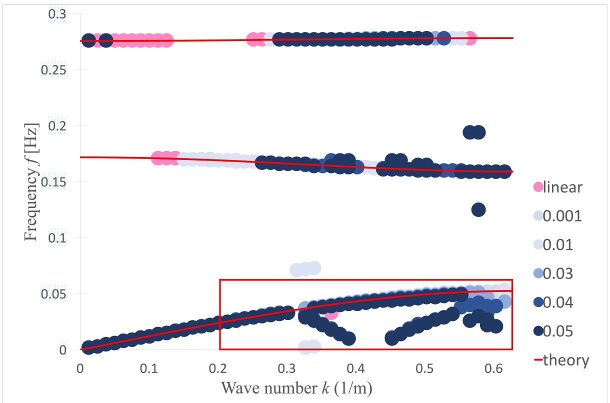

Figure 6: Results of nonlinear dynamics simulation: The number in the legend on the right of the graph indicates the magnitude of the amplitude and theorical dispersion curve in linear regime is shown as line.

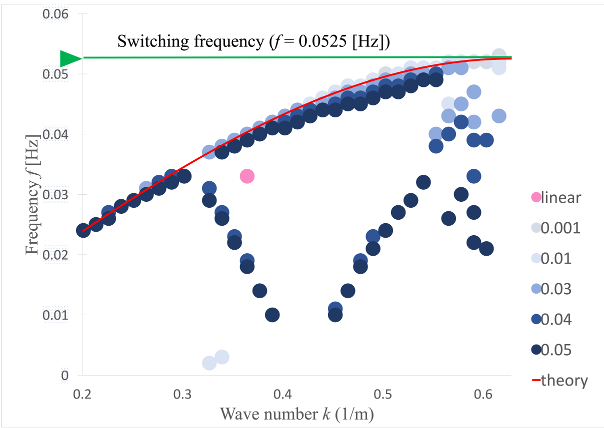

Figure 7: Results of nonlinear dynamics simulation near $f = 0.05$ [Hz]: f (on y axis) drops down as the amplitude of initial input increases.

applied to the model, which is given as

$$u_i(0) = a_0 \sin\left(j\frac{2\pi}{N}i\right), \tag{13}$$

where a_0 is amplitude of initial displacement and varies from $0.001l_0$ to $0.05l_0$, j varies from 1 to 50. We analyze how the behavior changes by increasing the amplitude of initial displacement. The results is shown in Fig. 6. In the lowest dispersion curve, the bifurcation is observed. Fig. 7 shows the results around $k = 0.2 - 0.6$[1/cm], $f = 0 - 0.06$ [Hz]. The results show that frequency components become smaller as the input amplitude increases than when the amplitude is small (Such as, $a_0 = 0.001l_0$.), or theoretical results in the linear regime (shown as line.). Thus, switching behavior is realized in the model around $f = 0.0525$ [Hz].

5. Conclusion

We construct the lattice model to reproduce the behavior of the PnCs and the SS, especially nonlinear behavior seen when the input amplitude is increased. This difference in the material property between the background and the scatterers is modelled by introducing the two types of mass point as well as the two types of springs. Moreover, in order to introduce nonlinearity in the model, mass of each mass points are changed in response to the displacement. In the linear dynamic simulation, the existence of band gap in the 1D and 2D model were confirmed. Finally, switching behavior was confirmed near $f = 0.0525$ [Hz] in the 1D model in nonlinear regime.

Acknowledgments

This work was supported by JSPS KAKENHI Grant Number 19K12003.

References

[1] G. Hu, L. Tang and J. Liang, C. Lan, and R. Das, “Acoustic-elastic metamaterials and phononic crystals for energy harvesting: A review,” Smart Mater. Struct., vol.30, num.8, 2021.

[2] Y. Pennec, J. Vasseur, B. Djafari-Rouhani , L. Dobrzyński, and P. Deymier, “Two-dimensional phononic crystals: Examples and applications,” Surf. Sci. Rep., vol.65, num.8, pp229-291, 2010.

[3] F. Motaei and A. Bahrami, “Nonlinear elastic switch based on solid–solid phononic crystals,” J. Mater. Sci., vol.55, num.21, pp.8983-8991, 2020.

[4] F. Motaei and A. Bahrami, “Two-channel all-elastic solid-solid phononic switch,” Phys. Scr., vol.95, num.6, 2020.

[5] F. Motaei and A. Bahrami, “Eight-channel acoustic demultiplexer based on solid-fluid phononic crystals with hollow cylinders,” Photonics Nanostructures: Fundam. Appl., vol.39, 2020.